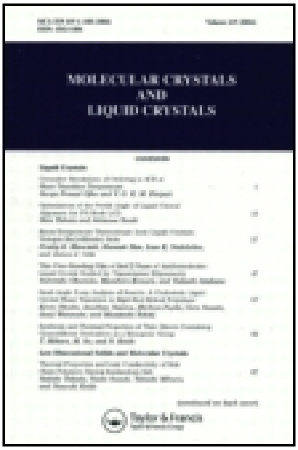

Molecular Crystals and Liquid Crystals
Publication details, including instructions for authors and subscription information:
http://www.tandfonline.com/loi/gmcl20

Fractal Features of Growing Aggregates from Isotropic Melt of a Chiral Bent-Core Liquid Crystal

Yuan Ming Huang [a] & Bao-Gai Zhai [b]
[a] College of Physics and Electronic Information, Yunnan Normal University, Kunming, Yunnan, China
[b] Modern Educational Technology Center, Yunnan Normal University, Kunming, Yunnan, China

Version of record first published: 05 Oct 2009

To cite this article: Yuan Ming Huang & Bao-Gai Zhai (2009): Fractal Features of Growing Aggregates from Isotropic Melt of a Chiral Bent-Core Liquid Crystal, Molecular Crystals and Liquid Crystals, 511:1, 337/[1807]-347/[1817]

To link to this article: http://dx.doi.org/10.1080/15421400903054444

Mol. Cryst. Liq. Cryst., Vol. 511, pp. 337/[1807]–347/[1817], 2009

ISSN: 1542-1406 print/1563-5287 online
DOI: 10.1080/15421400903054444

Fractal Features of Growing Aggregates from Isotropic Melt of a Chiral Bent-Core Liquid Crystal

Yuan Ming Huang[1] and Bao-Gai Zhai[2]
[1]College of Physics and Electronic Information, Yunnan Normal University, Kunming, Yunnan, China
[2]Modern Educational Technology Center, Yunnan Normal University, Kunming, Yunnan, China

Fractal features of aggregates growing out of the isotropic melt of a chiral bent-core liquid crystal, 1,3-phenylene bis {4-[3-chloro-4-(3,7-dimethyloctyloxyl)] phenyliminomethyl} benzoate, were investigated with differential scanning calorimetry, polarizing optical microscopy, and computer-aided simulation, respectively. Both star-like and grass-like aggregates were observed to grow out of the isotropic melt of the bent-core liquid crystal. With box-counting method, we calculated the fractal dimensions to be about 1.9 for both the star-like and the grass-like aggregates, suggesting the percolation growth of the banana-phase from the isotropic melt of the chiral bent-core liquid crystal.

Keywords: bent-core liquid crystal; chiral molecule; fractal aggregations; fractal dimension

1. INTRODUCTION

Bent-core liquid crystals (LCs) have attracted intensive attention because of their interesting ferro- and antiferroelectricity in the absence of molecular chirality [1–5]. Compared to their interesting electro-optical properties, the growth of the banana phases out of its isotropic melt has attracted little attention. Generally speaking,

Financial supports from the National Science Foundation of China (No. 10674091), the Scientific Research Fund for Returned Overseas Chinese Scholar from Education Ministry of China (No. 2005–546), and the Key Research Project of the Education Ministry of China (No. 206110) are gratefully acknowledged.

Address correspondence to Yuan Ming Huang, College of Physics and Electronic Information, Yunnan Normal University, No. 298, December 1st Street, Kunming, Yunnan 650092, China. E-mail: dongshanisland@126.com

the growth and aggregation have been topics of long-standing scientific interest in condensed-matter physics. Specifically speaking, the growth behaviors of the banana phases from isotropic melts of bent-core LCs are quite different from those of the smectic phases from isotropic melts of rod-like LCs [6,7]. For an example, nucleation and anisotropic growth of so-called bâtonnets is observed for rod-like LCs, in which growth perpendicular to the smectic layer plane is much more pronounced than growth in direction of the layer plane with the result of shape anisotropic aggregates. This means that the process of smectic layer formation is favored over the growth within individual layers. In contrast to the rod-like LCs, Dierking demonstrated that the complex growth structures of the achiral bent-core LC are qualitatively different from those exhibited by conventional calamitic phases [6,7]. The most prominent difference is that the aggregates exhibit the features of fractals for the bent-core LC 1,3-phenylene bis {4-[4-(octyloxyl)] phenyliminomethyl} benzoate. We have noticed that the bent-core LC studied by Dierking is achiral in itself.

In order to have a comprehensive understanding, the banana-phase growth behavior out of the melt of chiral bent-core LCs is of importance but such knowledge is not available in literature. A few years ago, Korean scientists Lee *et al*. synthesized a novel chiral bent-core LC 1,3-phenylene bis {4-[3-chloro-4-(3,7-dimethyloctyloxyl)] phenyliminomethyl} benzoate [8]. By means of differential scanning calorimetry, polarizing optical microscopy, triangular wave method and X-ray diffractometry, Lee *et al*. showed that this chiral bent-core LC exhibited antiferroelectric properties. In our work, we will select this chiral bent-core LC as a representative chiral bent-core LC for the investigations on the banana-phase growth behavior out of chiral bent-core LCs. Our results show that both star-like and grass-like fractal aggregates can be formed when the chiral bent-core LC undergoes phase transition from isotropic to banana phase at about 97°C. Detailed analysis on the features of the aggregates shows that the fractal dimensions of both the star-like and the grass-like aggregates are about 1.9.

2. EXPERIMENTAL DETAILS

Analytical reagents 8-bromo-2,6-dimethyl-2-octene, 4-nitro-2-chlorophenol, and benzene-1, 3-diol were purchased from Alfa Aesar, while analytical reagents 4-formyl-benzoic acid, triethylamine, ethyl acetate, pyridine and ethyl alcohol were purchased from Guanghua

Chemical Reagents Co. Ltd. (Guangdong, China). All reagents were used as received. Having followed the general synthetic methods [8–11], we had synthesized the chiral bent-core compound 1,3-phenylene bis {4-[3-chloro-4-(3,7-dimethyloctyloxyl)] phenyliminomethyl} benzoate. The synthesis route was schematically shown in Figure 1. The synthesized compound was purified by silica gel chromatography, and then was characterized with nuclear magnetic resonance (Bruker 400) and with Fourier transformed infrared spectroscopy, respectively. Our results were consistent with the data reported in Ref. [8]. Differential scanning calorimetry (Perkin Elmer-7) was used to characterize the phase transition of the synthesized compound. Both the heating rate and the cooling rate of the temperature were set to be 5°C/min. Using capillary method, the synthesized compound was filled into an LC cell whose spacing was measured to be about 4 μm. Indium-tin-oxide conducting electrodes were deposited onto the inner sides of the LC cell. An alternating voltage with triangular waveform was applied to the LC cell, and then the textures of the bent-core LC were recorded with a ppolarizing optical microscope (Aipha-Tech Ltd., China). A hot stage was used to regulate the temperature of the bent-core LC.

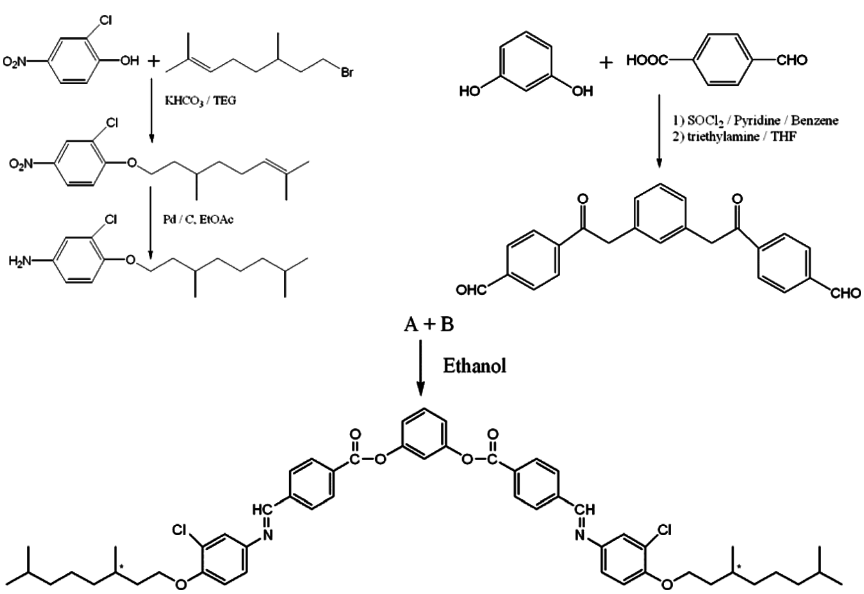

FIGURE 1 Synthesis route of the chiral bent-core liquid crystal 1,3-phenylene bis {4-[3-chloro-4-(3,7-dimethyloctyloxyl)] phenyliminomethyl} benzoate.

3. RESULTS AND DISCUSSION

The molecular structure of the bent-core LC is shown in Figure 1. According to the Cahn-Ingold-Prelog priority rules, we can determine the configuration of the bent-core molecule as *S*. Generally speaking, the chirality (R/S) of a molecule exhibits complicated relations to its optical properties. When optical activity is taken into consideration, for an example, the R/S chirality has no fixed relation to its (+)/(−) optical activity because an *R* enantiomer can rotates the light clockwise or counterclockwise, depending on its exact substituents. For chiral bent-core LCs, the general relations between the chirality of the molecules and their optical properties have not been firmly established due to limited investigations on chiral bent-core molecules.

Figure 2 shows the differential scanning calorimetry graphs of the chiral bent-core LC in the heating (above) and cooling (below) processes. Both the heating and cooling rates were fixed at 5°C/min. On heating, a broad appears at about 100°C while a sharp peak appears at about 97°C on cooling. On the basis of the heating and cooling curves in Figure 2, we can conclude that our chiral bent-core LC experiences a phase transition at about 97°C.

Figure 3 represents the polarizing optical micrographs of star-like aggregates growing out of the isotropic phase of the chiral bent-core LC. The temperature was fixed at about 97°C. The white areas in the panels of Figure 3 represent the banana-phase formed by the chiral bent-core LC while the black areas represent the isotropic phase of the LC. We define the moment as $t = 0$ when the banana phase

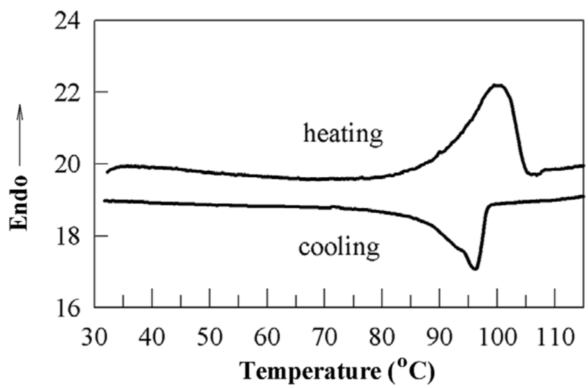

FIGURE 2 Differential scanning calorimetry graphs of the chiral bent-core liquid crystal in the heating (above) and cooling (below) processes. Both the heating and cooling rates were fixed at 5°C/min.

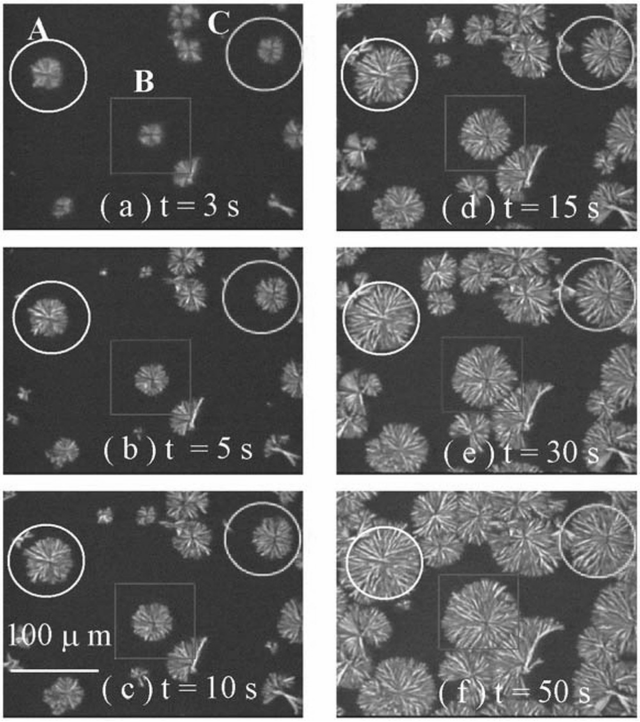

FIGURE 3 Time dependent polarizing optical micrographs of the star-like aggregates growing out of the isotropic phase of the chiral bent-core liquid crystal. The temperature was fixed at 97°C.

began to grow out of the isotropic phase. The micrographs in Figure 3 were taken at the time of $t = 3\,\mathrm{s}$ (panel *a*), $t = 5\,\mathrm{s}$ (panel *b*), $t = 10\,\mathrm{s}$ (panel *c*), $t = 15\,\mathrm{s}$ (panel *d*), $t = 30\,\mathrm{s}$ (panel *e*), and $t = 50\,\mathrm{s}$ (panel *f*), respectively. At a first glance, the star-like structures of the growing banana phase are self-similar. It is well known that self-similarity is a characteristic of fractals. For simplicity of quantitative analysis, three star-like structures of the growing banana phase are circled as A, B, and C in the panel *a*.

Quantitative analysis of the star-like structures in Figure 3 may provide useful information on the growth behavior of the banana phase for the chiral bent-core LC. Analysis of the patterns by fractal geometric methods has been proven a valuable tool in the description of complicated structures in many areas of science, ranging from physics, chemistry, and biology [12–15]. Fractal dimension is a measure of the irregularity of the boundary of an object, and our previous work demonstrated that the fractal dimension could be used to quantitatively characterize the surface roughness of films [13–15]. The box dimension of a fractal, D, is defined as

$$D = \lim_{\delta \to 0}\left[-\frac{\log N}{\log \delta}\right] \tag{1}$$

where N and δ are the counts of the boxes and the side lengths of the boxes, respectively. We can calculate the fractal dimension of an object by processing its polarizing optical micrographs. By means of box-counting method, we quantitatively analyzed the star-like structures of the growing banana phase from its isotropic melt, and the results are shown in Figure 4(a). Figure 4(a) represents the log-log plots of the counts of boxes against the side lengths of the boxes for the aggregates A, B, and C, respectively. By the definition of the fractal dimension in Eq. (1), the fractal dimension of an irregular surface equals to the absolute value of the slope of its log-log plot. Our calculated fractal dimensions are about 1.848, 1.849, and 1.890 for the star-like structures A, B, and C, respectively.

As shown in Figure 3, the star-like structures of the banana phase keep growing out of the isotropic melt of the chiral bent-core LC when the growth duration increases. In order to obtain the growth duration dependence of the fractal dimensions for the star-like structures, we calculated the fractal dimensions for the three typical structures A, B, and C at different growth stages. Figure 4(b) shows the growth-duration dependences of the fractal dimensions for the three typical structures A, B, and C, respectively. Our results in Figure 4(b) clearly demonstrate that the fractal dimensions are around 1.9 for the banana phase growing out of the isotropic melt of the chiral bent-core LC.

In addition to the star-like structures, grass-like growth of the banana phase was recorded for the chiral bent-core LC. Figure 5 shows the polarizing optical micrographs of the grass-like aggregates growing out of the isotropic melt of the chiral bent-core LC. The temperature was about 97°C. The white areas in the two panels of Figure 5 represent the banana-phase formed by the chiral bent-core LC while the black areas represent the isotropic phase of the LC. The growth time was 3 s for panel *a* and the growth time was 45 s for panel *b*, respectively. The fractal dimensions can also be calculated for these grass-like structures of the banana phase by performing similar data analysis as shown in Figure 4. Our calculated fractal dimensions are about 1.9 for those grass-like structures in Figure 5.

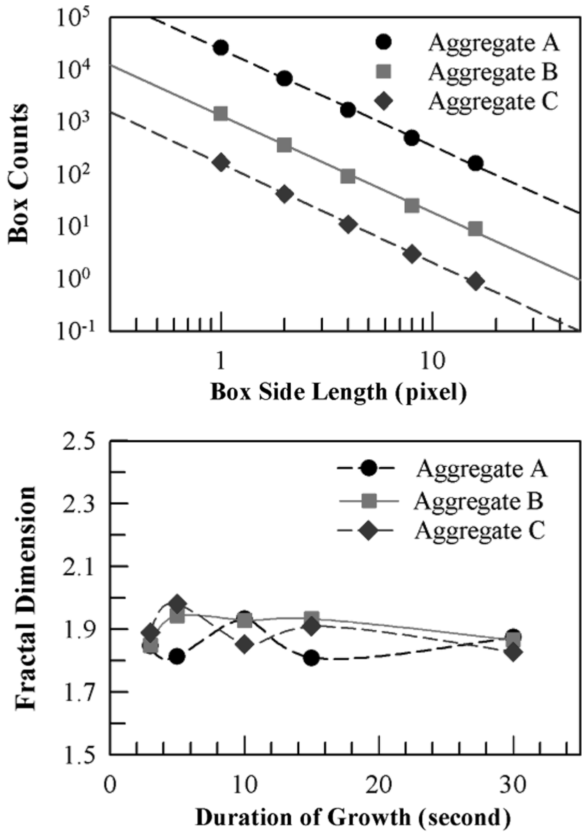

FIGURE 4 Log-log plots of the counts of boxes against the side lengths of the boxes for the aggregates A, B, and C, respectively. The box counting method was employed to calculate the fractal dimension of the aggregate.

Valuable information about the underlying growth mechanism can be extracted from the fractal dimensions of the star-like and grass-like structures for the chiral bent-core LC. As discussed in Refs. [6,7], there are three fundamental growth models: the diffusion-limited aggregation model, the cluster-cluster aggregation model and the percolation aggregation model. The model of diffusion-limited aggregation is based on single particles performing random walks before joining a single growing aggregate. The expected fractal dimension of such an aggregate is about 1.7 in two-dimensional space. Cluster-cluster aggregation involves the random motion of many particles at the same time, sticking together to form clusters which continue to perform

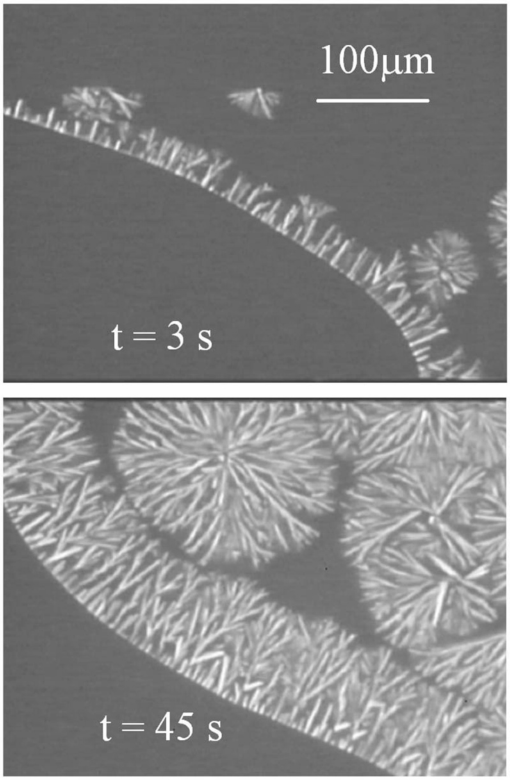

FIGURE 5 Time dependent polarizing optical micrographs of the grass-like aggregates growing out of the isotropic phase of the chiral bent-core liquid crystal. The temperature was fixed at 97°C.

random walks until eventually all particles are part of one single aggregate. The fractal dimension of cluster-cluster aggregation generally varies between 1.6 and 1.8 in two-dimensional space, depending strongly on experimental conditions. The percolation model is to take a regular lattice and make it into a random network by randomly "occupying" sites (vertices) or bonds (edges) with a statistically independent probability p. At a critical threshold p_c, long-range connectivity first appears. A fractal dimension of 1.896 is theoretically expected for the percolation aggregation. Values of our calculated fractal dimensions for the fractal structures of the banana phase suggest that the growth process of the banana phase can be described by the percolation aggregation model. In the framework of percolation aggregation model, we simulated the growth of the banana phase out of its

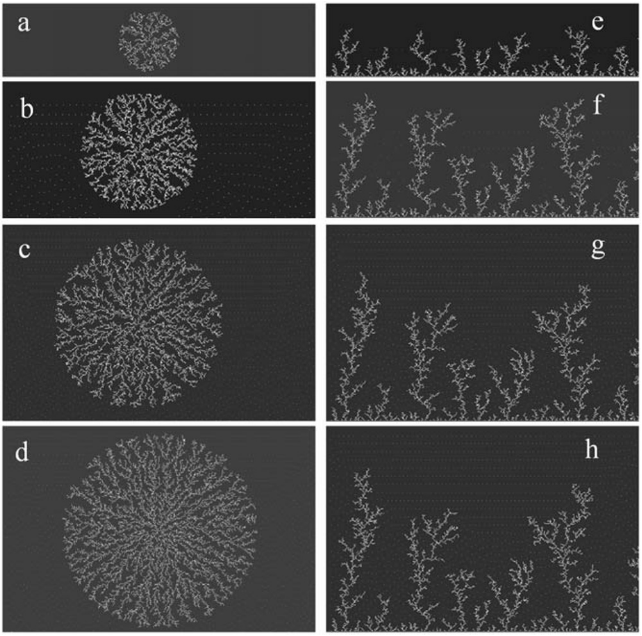

FIGURE 6 Simulated growth aggregate for the star-like aggregates and grass-like aggregates out of the isotropic phase of the chiral bent-core liquid crystal.

isotropic melt of the chiral bent-core LC. The simulated star-like fractals and grass-like fractals are shown in Figure 6. It is obvious that our simulated growth behaviors are very similar to those depicted in Figures 3 and 5.

As depicted in Figures 3 and 5, the chiral bent-core molecules sometimes form star-like aggregates and sometimes form the grass-like aggregates. The growth of a solid film on a substrate generally takes place in the mode of island growth, and the atomic features and defect formations on the surfaces of a LC cell are believed to play a key role in the pattern formation of the fractals. The inner surfaces of our LC cell were coated with thin layers of polyimide and then unidirectionally rubbed. The numerous fine particles and debris left on the surfaces of a LC cell may act as nuclei for the crystallization of the bent-core molecules. Once the nucleation islands are sparsely distributed on the inner surfaces of our LC cell, subsequent crystal growth should occur randomly near the well-separated nucleation islands. As a result, star-like aggregates will be developed. If the nucleation islands are densely distributed on the surfaces of a LC cell, some neighboring islands will inevitably form a chain of islands, and the subsequent crystal growth should occur along the chain of the nucleation islands. As a result, grass-like aggregates can be developed.

An alternating electric field can induce loss in the birefringence of both the star-like structures and the grass-like structures of the banana phase for the chiral LC. Our experimental results demonstrated that the electric field (20 $V_{pp}/\mu m$, 1 Hz) could turn the birefringent aggregates into dark [16,17]. To understand the origin of the loss in the birefringence of the chiral bent-core LC, we measured the conductivity measurement and dielectric constants of the LC, and our results indicated that the ions in the chiral bent-core LC are responsible for the electrically induced loss in the birefringence of the chiral bent-core LC.

4. CONCLUSION

With differential scanning calorimetry, polarizing optical microscopy and computer-aided simulation, we have investigated the fractal features of aggregates growing out of the isotropic melt of a chiral bent-core LC 1,3-phenylene bis {4-[3-chloro-4–3,7-dimethyloctyloxyl]}-phenyliminomethyl}benzoate. When the chiral bent-core LC cools from its isotropic phase to its banana phase, both star-like aggregates and grass-like aggregates can be formed. With box-counting method, we have calculated the fractal dimensions for the star-like and grass-like aggregates. Our results have demonstrated that the fractal dimensions of the two kinds of aggregates are independent of their growth duration. Our growth simulation and the calculated values of the fractal dimensions suggest that the percolation aggregation model can be applied to the processes of the banana-phase growing out of its isotropic melt of the chiral bent-core liquid crystal.

REFERENCES

[1] Niori, T., Sekine, T., Watanabe, J., *et al.* (1996). *J. Mater. Chem.*, *6*, 1231.
[2] Sekine, T., Niori, T., Sone, M., Watanabe, J., Choi, S. W., Takanishi, Y., & Takazoe, H. (1997). *Jpn. J. Appl. Phys.*, *36*, 6455.
[3] Dierking, I. (2001). *Chem. Phys. Chem.*, *2*, 59.
[4] Heppke, G. & Moro, D. (1998). *Science*, *279*, 1872.
[5] Link, D. R., Natale, G., Shao, R., *et al.* (1998). *Science*, *278*, 1924.
[6] Dierking, I. (2001). *Physica B*, *304*, 51.
[7] Dierking, I., Chan, H. K., Culfaz, F., McQuire, S. (2004). *Phys. Rev. E*, *40*, 051701.
[8] Lee, C. K., Kwon, S. S., Kim, T. S., Choi, E. J., Shin, S. T., Zin, W. C., Kim, D. C., Kim, J. H., & Chien, L. C. (2003). *Liq. Cryst.*, *30*, 1401.

[9] Hassner, A. & Alexanian, V. (1978). *Tetrahedron Lett.*, *19*, 4475.
[10] Gray, G. W. & Jones, B. (1954). *J. Chem. Soc.*, 1467–1470.
[11] Kuhn, W. E. (1943). *Org. Synth. Collect.*, *2*, 447.
[12] Mandelbrot, B. (1982). *The Fractal Geometry of Nature*, Freeman: San Francisco.
[13] Huang, Y. M., Zhai, B. G., & Zhou, F. F. (2008). *Appl. Surf. Sci.*, *254*, 4139.
[14] Huang, Y. M. & Zhou, F. F. (2006). *Spectroscopy and Spectral Analysis*, *27*, 762.
[15] Zhou, F. F. & Huang, Y. M. (2007). *Appl. Surf. Sci.*, *253*, 4507.
[16] Huang, Y. M., Chen, L., Zhou, F. F., & Zhai, B. G. (2007). In: *New Trends in Fluid Mechanics Research*, Zhuang, F. G. & Li, J. C. (Eds.), Tsinghua University Press & Springer: Beijing, 61.
[17] Huang, Y. M. (2005). In: *Trends in Optics and Photonics Series: Photorefractive Effects, Materials, and Devices*, Zhang, G., Kip, D., Nolte, D., & Xu, J. (Eds.), Optical Society of America: Washington, Vol. 99, 288.